ELSEVIER

Journal of Food Engineering 62 (2004) 185–192

JOURNAL OF FOOD ENGINEERING

www.elsevier.com/locate/jfoodeng

Intrinsic and relative permeability for flow of humid air in unsaturated apple tissues

H. Feng [a], J. Tang [b,*], O.A. Plumb [c], R.P. Cavalieri [b]

[a] Department of Food Science and Human Nutrition, University of Illinois at Urbana-Champaign, Urbana, IL 61801, USA
[b] Department of Biological Systems Engineering, Washington State University, 213 L J Smith Hall, Pullman, WA 99164-6120, USA
[c] College of Engineering, Box 3295, University of Wyoming, Laramie, WY 82071, USA

Received 1 July 2000; received in revised form 30 September 2002; accepted 4 June 2003

Abstract

Knowledge of intrinsic and relative permeabilities is important when studying pressure driven mass transport in unsaturated porous media. Little information is available on intrinsic and relative permeabilities of biomaterials. In this study, an experimental procedure was developed to determine intrinsic and relative permeabilities for the flow of humid air in porous apple tissues. Experiments were completed in two steps. In the first step, apple tissues were freeze-dried to remove moisture without changing the sample's original pore structure. Dry air was passed through the sample and Darcy's law was used to determine intrinsic permeability, K, as a function of porosity. In the second step, moist air was forced through partially saturated apple tissues to determine the air permeability, K_g. The humid air was in thermodynamic equilibrium with the apple tissues to obtain an equivalent immiscible condition. The air relative permeability k_{rg} was then calculated based on the value of the air permeability K_g and the intrinsic permeability K. The intrinsic permeability for apple tissue varied from 8.89×10^{-13} to 4.57×10^{-11} m^2 for porosity ranging from 0.33 to 0.77. The porosity dependency of intrinsic permeability can be described by the Kozeny–Carman model. The gas relative permeability k_{rg} was correlated to saturation by an empirical model.

Keywords: Relative permeability; Intrinsic permeability; Porous media; Kozeny–Carman model; Mass transfer

1. Introduction

Multi-phase flow in unsaturated porous media is of practical importance in many industrial applications, including steam enhanced extraction for removing liquid contaminants, treating leachate in bioreactors, flow in the vadose zone, and drying biomaterials in the falling rate periods. The single-phase Darcy's law has been extended to quantify multi-phase flow problems by introducing a relative permeability for each phase. In an immiscible two-phase flow, the flow of one fluid is assumed to behave as though it coexists with another fluid in a stationary state. The effective porosity for the fluid flow is reduced to its volume fraction, and the fluid velocity is correspondingly less than a single-phase situation by a factor between 0 and 1 (Dullien, 1979). This factor is referred to as the relative permeability. For a gas–liquid flow, the permeability for gas flow K_g is a product of the intrinsic permeability K and the gas relative permeability k_{rg} while the permeability for liquid flow K_l is a product of K and the liquid relative permeability k_{rl} where K is an intrinsic property of pore structure and k_{rg} & k_{rl} is a function of liquid saturation. Knowledge of intrinsic and relative permeability is essential for characterizing muiti-phase flow in an unsaturated porous medium.

Extensive studies on permeability determination for single- and multi-phase flows have been performed in the fields of soil physics (Moldrup, Poulsen, Schjønning, Olsen, & Yamaguchi, 1998; Stylianou & DeVantier, 1995), petroleum production (Johnson, Bossler, & Naumann, 1958), and wood processing (Choong, Tesoro, & Manwiller, 1974; Rice & D'Onofrio, 1996; Tesoro, Choong, & Kimbler, 1974). Several researchers have provided extensive reviews on techniques used to determine permeability (Avraam & Payatakes, 1995; Dullien, 1979; Honarpoor & Mahmood, 1988). In single-phase permeability determination, both gaseous and liquid

* Corresponding author. Tel.: +1-509-335-2140; fax: +1-509-335-2722.
E-mail address: jtang@mail.wsu.edu (J. Tang).

0260-8774/$ - see front matter © 2003 Elsevier Ltd. All rights reserved.
doi:10.1016/S0260-8774(03)00231-0

Nomenclature

A	cross-sectional area, m^2
C_0	Kozeny constant
D_P	mean equivalent diameter of the flow path, m
$\overline{D}$	effective average grain or fiber diameter, m
H	specimen thickness, m
k_{rg}, k_{rl}	relative permeability of gas and liquid phase, respectively
K	intrinsic permeability, m^2
K_g, K_l	pas and liquid phase permeability, m^2
Q_g	flowrate of air into specimen, m^3/s
P_g	specimen pressure drop, Pa
RH	relative humidity
S	liquid saturation
S_v	specific internal area, 1/m
T	test temperature, K
u	velocity, m/s
V	volume, m^3
X	moisture content, kg H_2O/kg dry solid

Greek letters

ε	porosity, void volume/total volume
ε'	porosity, gas volume/total volume
μ	viscosity, kg/(m s)
ρ	density, kg/m^3

Subscripts

a	air
g	gas
l	liquid
s	solid
w	water

media can be used. Since ideal single-phase flow is seldom encountered in most applications, a common practice is to identify a dominant phase and to measure the permeability for this flow (Choong et al., 1974). Goedeken and Tong (1993) measured the gas permeability of bread with an airflow apparatus. Eischens and Swanson (1996) proposed an ASTM method for the determination of the pneumatic permeability of partially saturated porous materials based on an airflow test. The pneumatic permeability they measured was the averaged gas permeability K_g. Permeability of an unsaturated porous medium measured using single-phase tests is commonly referred to as apparent or effective permeability. In the study of multi-phase flow problems, however, it is necessary to separate the flow of each phase by introducing intrinsic and relative permeabilities. The effective permeability measured using single-phase tests does not provide information about intrinsic and relative permeabilities in flows in unsaturated media.

For multi-phase flows, relative permeabilities can be determined experimentally using steady state or unsteady state methods (Berge, Gjertsen, & Lysne, 1998; Honarpoor & Mahmood, 1988). Determination of relative permeabilities using hypothetical structural models has also been widely used (Honarpoor & Mahmood, 1988; Plumb, 1991). The steady or unsteady state methods, although having some limitations (Couture, Jomaa, & Puiggali, 1996), have been used to determine the permeability of two immiscible fluids in soil and in petroleum bearing materials. In spite of considerable study of immiscible flow problems, the question of how to determine relative permeability for two-phase flows that consist of water and humid air remains unanswered (Couture et al., 1996). It is difficult to directly apply the techniques developed for immiscible flow problems to study water–air flows. One reason is that the humid air and liquid phase are no longer immiscible. Local saturation may change during the course of measurements. In addition, stratification caused by density differences between air and water may create a major problem. That is, air may flow predominantly in one region of a porous medium while liquid flows may predominate in other regions. This stratification causes difficulty in an experimental design. Because of the above-mentioned difficulties, there exists little literature on measured intrinsic and relative permeabilities for humid air–water flow problems.

Relative permeability is an important parameter in analyzing mass transport in biomaterials. One example is the microwave drying of foodstuffs where significant internal vapor pressure may develop as a result of volumetric dielectric heating. The flow driven by the pressure gradient as described by the generalized Darcy's law is a dominant transport mechanism in some stages of microwave or radio frequency drying (Feng, 2000). However, relative permeability data for the migration of water and humid air in biomaterials do not exist in the literature. The purpose of this study is (1) to develop an experimental procedure to measure both the intrinsic and relative permeability of apple tissues based on a gaseous phase test, and (2) to study the influence of porosity and saturation on intrinsic and relative permeabilities.

2. Theory

For gas–liquid flow in an unsaturated porous medium, the gas and liquid velocities can be estimated by the generalized Darcy's law (Nield & Bejan, 1999):

$$\vec{u}_g = -\frac{K_g}{\mu_g}(\nabla P_g - \rho_g \vec{g}) = -\frac{K(\varepsilon)k_{rg}}{\mu_g}(\nabla P_g - \rho_g \vec{g}) \qquad (1)$$

$$\vec{u}_l = -\frac{K_l}{\mu_l}(\nabla P_l - \rho_l \vec{g}) = -\frac{K(\varepsilon)k_{rl}}{\mu_l}(\nabla P_l - \rho_l \vec{g}) \quad (2)$$

where $K(\varepsilon)$ is the intrinsic permeability at porosity ε, and K_i, k_{ri}, μ_i, and ρ_i are permeability, relative permeability, viscosity, and density for gas ($i = g$) and liquid ($i = l$). The gravitational term in Eqs. (1) and (2) can be ignored compared to the pressure term for appropriate conditions. The application of Darcy's law requires that two fluids are immiscible. The flow also needs to be laminar and at a steady state (Berge et al., 1998). Since Eqs. (1) and (2) are valid at the representative elementary volume level, an accurate estimation of local permeabilities requires knowledge of both velocity and pressure fields at the REV scale. However, the velocity and pressure distributions are usually unknown and need to be determined. A commonly used approach is to directly apply Darcy's law to evaluate the permeabilities at a macro-scale level by considering an average flow (Berge et al., 1998; Eischens & Swanson, 1996). This approach was used in the present study. Consider a one-dimensional horizontal gas–liquid flow through an unsaturated cylindrical specimen of thickness H. The average gas velocity can be written as

$$\bar{u}_g = -\frac{K_g}{\mu_g}\frac{\Delta P_g}{H} = -\frac{K(\varepsilon)k_{rg}}{\mu_g}\frac{\Delta P_g}{H} \quad (3)$$

where ΔP_g is pressure drop across the sample. The gas flowrate Q_g is related to ΔP_g by

$$Q_g = \bar{u}_g A = -A\frac{K_g}{\mu_g}\frac{\Delta P_g}{H} = -A\frac{K(\varepsilon)k_{rg}}{\mu_g}\frac{\Delta P_g}{H} \quad (4)$$

where A is the cross-section area of the specimen. Permeabilities defined in Eq. (4) are averaged values over the specimen thickness. From Eq. (4), it can be seen that the gas permeability $K_g = K(\varepsilon)k_{rg}$ can be evaluated from the measurement of Q_g and ΔP_g.

In this study, a procedure was developed based on a gas flow test to determine intrinsic permeability, $K(\varepsilon)$, and relative permeability, k_{rg}, for a humid air–water flow problem. The experiment consisted of two steps. In the first step, the intrinsic permeability $K(\varepsilon)$ was determined as a function of porosity. This was done by passing dry air through a dry sample in which $k_{rg} = 1$. The gas permeability K_g thus determined was intrinsic permeability $K(\varepsilon)$ at porosity ε. The intrinsic permeability was also measured with dry samples of various porosity to establish a relationship between $K(\varepsilon)$ and ε.

The gas relative permeability k_{rg} was determined in the second step by humid-air/moist-sample tests. In the tests, if Darcy's law applies, from the slope of a flowrate and pressure drop curve we can find the gas permeability K_g using Eq. (4). The gas relative permeability k_{rg} was then evaluated from

$$k_{rg} = \frac{K_g(\varepsilon, S)}{K(\varepsilon)} \quad (5)$$

In Eq. (5) the intrinsic permeability $K(\varepsilon)$ has been determined in the first step.

An effort was made to maintain the conditions under which Darcy's law can be applied. This was done by controlling the air humidity to achieve an equivalent immiscible humid air–water flow condition. The air was humidified to a relative humidity in equilibrium with the moist sample according to sorption relations. When passing the humid air through moist samples, local saturation remained unchanged and hence an immiscible condition was considered satisfied. The stable flow condition was maintained by controlling and monitoring the air flowrate. With the above conditions maintained, the movements of humid air and water can be considered to be independent. Whether the water phase is flowing or stationary, we can use an airflow test to determine the permeabilities for the air phase. A major advantage of this approach is that stratification at the specimen scale can be avoided. The flow at pore level is equivalent to a humid air–water flow with a water fraction represented by its saturation level.

Special care needs to be taken when applying Eq. (5). For many biomaterials, porosity changes with degree of saturation because of the shrinkage associated with removal of moisture. As a result, a material at a different saturation level will have different porosity, and hence different intrinsic permeability. The relationship between porosity and saturation must first be established in order to obtain the intrinsic permeability $K(\varepsilon)$. When the gas relative permeability is determined, the liquid relative permeability k_{rl} can be obtained using selected empirical relations.

3. Experimental

3.1. Measurement system

An experimental apparatus was developed to measure the flowrate of moist air and the pressure drop across the sample (Fig. 1). The air temperature and humidity were adjusted by an air humidifier, a low temperature water bath, and a high temperature water bath. For a given moist apple sample, we can find an equilibrium air relative humidity according to sorption relations (Roman, Urbicain, & Rotstein, 1982). The low temperature water bath was set at the dew point temperature to ensure the air was saturated. The high temperature water bath was used to raise the temperature to room temperature at required relative humidity. Other components in the system included an airtight cylindrical sample holder, a flowmeter to measure air flowrate, and a manometer to measure pressure drop.

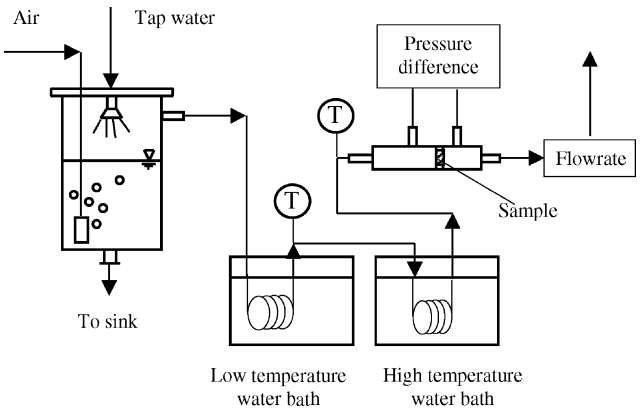

Fig. 1. Setup for permeability determination.

3.2. Specimen preparation

Red Delicious apples were cored, peeled, and sliced into slabs 10–15 mm thick. The slabs were cut parallel to the stem–calyx axis of the apple. Apple slabs were freeze-dried in a Freezemoble 24-Unitop freeze dryer (Virtis Company, Gardiner, NY) to a moisture content of <6% (dry basis). The freeze-dried samples were considered dry. The dry samples maintained the pore structure of fresh apples and were used in the single-phase tests to determine the intrinsic permeability. Freeze-dried apples were also conditioned to two moisture contents for use in moist air tests. Cylindrical wafers (14 mm in diameter and 3.5 mm thick) were cut from the freeze-dried slabs for the permeability determination. The flow through the wafers was then in the radial direction of the apple.

The specimen size was selected so that each specimen contained adequate cells. A typical parenchyma cell in Delicious apple tissue has a diameter of 165.5 ± 28.5 μm. The intercellular spaces are typically 269.0 ± 93.0 μm (width) and 487.8 ± 154.0 μm (length) (Mohsenin, 1986). In a 3.5 mm thick specimen, there were about 20 repeated cells units. The sample thickness, therefore, was considered adequate to represent a typical apple tissue on the macro-scale.

3.3. Experimental procedure

3.3.1. Intrinsic permeability

The specimen was placed in a sample holder specially designed to maintain good sealing during the tests. Vacuum grease was applied at the edge of the specimen. Dry air was forced through the sample and measurements were made after a steady flow condition was achieved. Since for dry air/dry sample tests, $k_{rg} = 1$, the intrinsic permeability can be calculated from the slope of the air flowrate versus pressure gradient curve as described in Eq. (4). The measurements were conducted in seven replicates and the mean was reported.

Sample porosity was changed by pressing the freeze-dried apple slabs into different thicknesses. The intrinsic permeability $K(\varepsilon)$ was determined as a function of porosity ε. Due to the difficulty in obtaining specimens with a known porosity, measurements were conducted at thirteen different porosity values without replication.

3.3.2. Relative permeability

The freeze-dried wafers were conditioned in desiccators with saturated NaCl and KCl solutions which provided a relative humidity of 75.3% and 84.3%, respectively. Two relative humidity values provided storage conditions to adjust the samples to two different saturation levels. When equilibrium was reached, moisture contents of the samples in two containers were 36.0% and 60.0% (db), respectively. Samples with moisture content greater than 60% (db) were not used in the tests because samples were too soft to withstand the pressure difference without changing structure. In order to prevent changes in saturation during a measurement, moist air with a relative humidity (RH) in equilibrium with the apple sample's moisture content was used. That is, for samples with moisture of 36.0% (db), air with relative humidity of 75.3% was used, while for moisture of 60.0% (db), the relative humidity was set at 84.3%.

Nine replicates were measured at a moisture level of 36.0% (db). At a moisture content of 60.0% (db), the apple specimens became soft and difficulties were experienced in obtaining reliable readings. Large deformation took place when flowrate and the pressure drop were high. This caused either the sealing to fail or an incorrect reading. For this reason, only three replicates were conducted at a moisture content of 60% (db).

Moisture content affects sample porosity and, hence, intrinsic permeability $K(\varepsilon)$. For apples, a porosity–moisture relation was derived based on data reported by Lozano, Rotstein, and Urbicain (1980):

$$\varepsilon' = \frac{V_a}{V_a + V_w + V_s} = 1 - \frac{0.852 - 0.462\exp(-0.66X)}{1.54\exp(-0.051X)} \quad (6)$$

where X is moisture content on a dry basis. The porosity ε' given by Eq. (6) was defined as the ratio of air void to total volume. It needs to be converted to porosity ε used in multi-phase flow studies, which equals total void (gas void + void occupied by water) over total volume:

$$\varepsilon = \frac{V_a + V_w}{V_a + V_w + V_s} = \frac{\varepsilon' + \rho_s X/\rho_l}{1 + \rho_s X/\rho_l} \quad (7)$$

where $\rho_s = 1650$ kg/m^3 (Krokida & Maroulis, 1999) is the solid density of apples. Substituting Eq. (6) into (7) results in,

$$\varepsilon = \frac{1}{1 + 1.65X}\left[\left(1 - \frac{0.852 - 0.462\exp(-0.66X)}{1.5\exp(-0.051X)}\right) + 1.65X\right] \quad (8)$$

Eq. (8) is the porosity–moisture relation for apples. It was used to calculate porosity values for samples with moisture contents between 36% and 60% (db). The calculated porosity values were then used to determine the intrinsic permeability $K(\varepsilon)$ using the $K(\varepsilon)$–ε relation obtained in the intrinsic permeability experiments. The gas relative permeability k_{rg} can then be evaluated from K_g using Eq. (5).

4. Results and discussions

4.1. Intrinsic permeability and effect of porosity

Fig. 2 illustrates a typical air velocity versus pressure gradient curve. It can be seen that when air velocity was less than about 0.1 m/s, a linear relation existed, and hence Darcy's flow condition applied. The least square method was used to fit data in the linear range to a straight line that passes through the origin. The intrinsic permeability was determined from the slope of the straight line.

The flow in apple tissues can be characterized using the hydraulic radius theory (Greenkorn, 1983). If the cellular structure in apples can be treated as a packed bed of spherical grains, the Reynolds number for porous apple tissues can be written as

$$Re = \frac{4R_H v_\infty \rho}{\varepsilon \mu} \tag{9}$$

where v_∞ is velocity of approaching fluid, and R_H is hydraulic radius, which is given by (Baijal, 1982)

$$R_H = \frac{D_P}{6}\frac{\varepsilon}{1-\varepsilon} \tag{10}$$

where D_P is the mean equivalent diameter of the flow path in apples. For Delicious apples, D_P was 362 μm, calculated from the size of the intercellular spaces given by Mohsenin (1986). Substituting Eq. (10) into Eq. (9), we obtain a Reynolds number for porous apples as follows:

$$Re = \frac{2}{3(1-\varepsilon)}\frac{D_P v_\infty \rho}{\mu} \tag{11}$$

The Reynolds number for flow in apple tissues was presented as a function of pressure gradient in Fig. 2. Generally, Darcy's law is valid in the creeping flow region where Re is less than 1.0 (Greenkorn, 1983). From Fig. 2, the linear relation holds until Re reaches about 4.0. After that point, the deviation increases with air velocity and becomes significant when $Re > 6.0$. The fact that the linear relation extended to $Re > 1.0$ may be attributed to inaccurate estimation of the mean equivalent diameter D_P and the geometric assumption of spherical packed grains to simulate apple tissues.

The measured intrinsic permeability $K(\varepsilon_0)$ for freeze-dried intact apple tissues was 4.57×10^{-11} ($\pm9.0\times10^{-12}$) m^2. This value was compared with data reported in the literature for bioproducts (Table 1). It can be seen that the intrinsic permeability of apple tissues falls in the range of the intrinsic permeability of cork board. $K(\varepsilon_0)$ of apples is lower but at the same magnitude when compared to the intrinsic permeability of hard wood. However, apple tissue has a much higher intrinsic permeability compared to that of soft wood.

Cork is a wood tissue composed of hollow dead cells. It has a low bulk density ρ_b (120–160 kg/m^3) (Ordovás, Carmona, Moreno, & Ortega, 1996). Ordovás et al. reported that the solid density ρ_s of cork is 1500 kg/m^3. Hence, when the moisture content of the cork is very low and can be ignored, the porosity ε of cork can be calculated from the bulk density ρ_b and solid density s. Calculated porosity for cork varied from 0.89 to 0.92 and was larger than the porosity of apple tissue ($\varepsilon = 0.77$). A specific feature of the cork is its occluded internal pores, which do not provide passages to fluid flow. Experiments conducted by Ordovás et al. revealed that about 10% of the pores in corks were closed. The effective porosity of the cork is then in the range of 0.80–0.83. This may explain why the measured intrinsic permeability of apples was close to the reported values for cork.

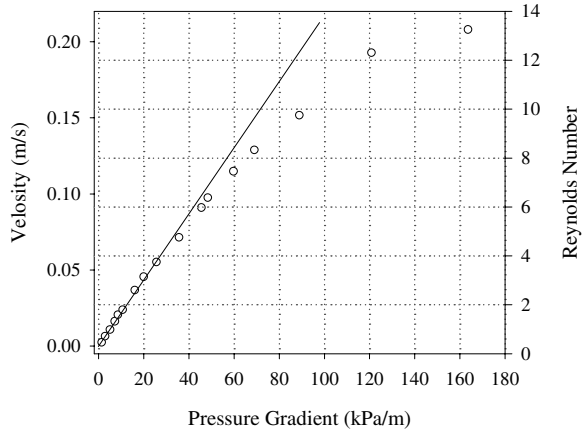

Fig. 2. Linear range on an air velocity versus pressure gradient plot as influenced by Reynolds number (porosity $\varepsilon = 0.77$, room temperature, dry sample).

Table 1
Intrinsic permeability data of selected biomaterials

Material	Intrinsic permeability K (m^2)	Reference
Hard wood	1.95×10^{-11}[a]	Choong et al. (1974)
Soft wood	1×10^{-13}[b]	Perré and Turner (1999)
Cork board	$(2.4–5.7)\times10^{-11}$	Nield and Bejan (1999)
Apple tissue	4.57×10^{-11}	Present study

[a] Mean of longitudinal direction gas permeabilities of 22 hardwoods at 0% moisture content.
[b] Longitudinal direction.

4.2. Kozeny–Carman model for intrinsic permeability

Fig. 3 presents measured intrinsic permeabilities at different porosities. It is desirable to approximate the data mathematically if it is to be useful in simulating a drying process. The intrinsic permeability of a material is determined by its pore structure. Therefore, one can estimate intrinsic permeability for simplified structures using the theory of fluid mechanics. Several models have been developed using this approach (Dullien, 1979). Kozeny's equation and various modified forms are among the most popular models. The Kozeny equation was derived using the hydraulic radius to represent the flow passages and assuming the porous medium to be composed of a bundle of tortuous capillaries. A general expression of Kozeny's equation can be written as (Baijal, 1982)

$$K(\varepsilon) = \frac{C_0}{S_v^2}\frac{\varepsilon^3}{(1-\varepsilon)^2} \tag{12}$$

where C_0 is the Kozeny constant and S_v is specific internal area. Carman (1937) obtained a C_0 of 0.2 based on experimental results. For spherical grain porous media, $S_v = 6/\overline{D}$. Thus Eq. (12) reduces to the Kozeny–Carman model (Nield & Bejan, 1999):

$$K(\varepsilon) = \frac{\overline{D}^2}{180}\frac{\varepsilon^3}{(1-\varepsilon)^2} \tag{13}$$

where $\overline{D}$ is effective average grain or fiber diameter.

The intrinsic permeability data of apple tissues were fitted to the Kozeny–Carman model to obtain

$$K(\varepsilon) = 5.578\times10^{-12}\frac{\varepsilon^3}{(1-\varepsilon)^2} \quad (0.39 < \varepsilon < 0.77;\ R^2 = 0.95) \tag{14}$$

The correlation coefficient for this fit was 0.95 and the standard deviation for the coefficient is 0.259×10^{-12}. From Eq. (14) the effective average grain diameter was estimated to be 100.2 μm. This value is close to the lower limit of the parenchyma cell diameter of Delicious apple tissues, 137.0 μm (Mohsenin, 1986). The discrepancy might be caused by the geometry difference between the apple tissue and the assumption made in the Kozeny–Carman model.

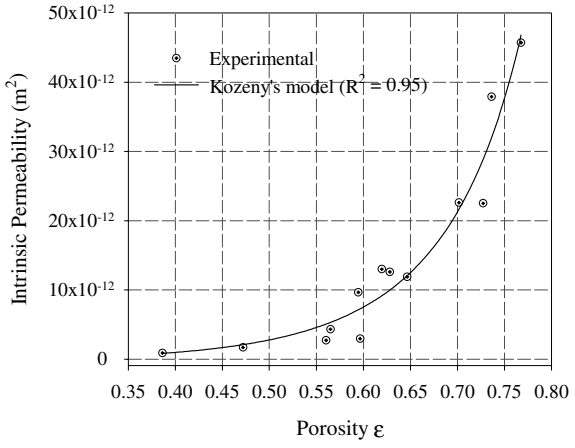

Fig. 3. Intrinsic permeability of apple tissues as a function of porosity.

4.3. Relative permeabilities

The relative permeabilities for apple tissues corresponding to moisture contents of 36.0% (db) and 60.0% (db) are presented in Fig. 4. At a moisture level of 36.0% (db), the gas permeability K_g was $7.4\times10^{-12}\pm1.2\times10^{-12}$ m^2 and gas relative permeability k_{rg} was 0.44 ± 0.05. At a moisture content of 60.0% (db), the gas permeability was $6.5\times10^{-13}\pm2.4\times10^{-13}$ m^2 and gas relative permeability was 0.05 ± 0.01. The sharp decrease in the gas permeability when moisture increases from 36% (db) to 60% (db) is an indication of an increase in the resistance to the humid air flow. This might also be caused by errors in estimating porosity of apple samples under absorption conditions using Eq. (8), which is from dehydration tests. The use of Eq. (8) might have overestimated the porosity that resulted in a larger intrinsic permeability K, and hence an underestimated gas relative permeability k_{rg}.

It is desirable to develop a mathematical expression to correlate the gas relative permeability k_{rg} to liquid saturation S. Numerous studies have been carried out to develop such an expression (Plumb, 1991). The forms of the expressions depended upon pore structure (Perré & Turner, 1997). A widely used assumption was that the liquid phase is not continuous when saturation is lower than a certain value. Saturation at this value was known as the irreducible saturation S_{irr}. The relative permeability, therefore, needs to be expressed using two different expressions for saturation $S < S_{irr}$ and $S > S_{irr}$.

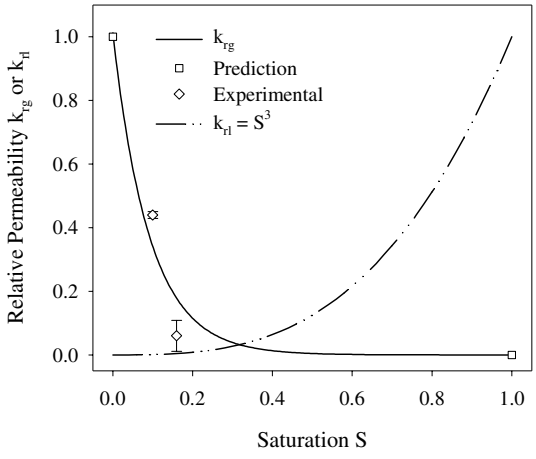

Fig. 4. Humid air (k_{rg}) and water (k_{rl}) relative permeabilities of apple tissues as a function of saturation.

Couture et al. (1996) suggested that for hygroscopic porous media, the introduction of S_{irr} resulted in a mathematical singularity. It is difficult to differentiate between the flow of continuous free water and bound water if a discontinuous free water flow regime exists. In this study, the concept of S_{irr} was not used and the saturation of freeze-dried apples was assumed to be zero. Therefore, air and water relative permeability k_{rg} and k_{rl} are defined as

$$\begin{aligned} &\text{when } S = 0; \quad k_{rg} = 1 \text{ and } k_{rl} = 0 \\ &\text{when } S = 1; \quad k_{rg} = 0 \text{ and } k_{rl} = 1 \end{aligned} \tag{15}$$

An empirical relation was obtained using both the experimentally determined relative permeability values and the values defined at $S = 0$ and 1. The correlation is written as

$$k_{rg} = 1.01e^{-10.86S} \quad (0 < S < 1;\ R^2 = 0.96) \tag{16}$$

where S is liquid saturation. The liquid relative permeability k_{rl} is expressed by the widely used cubic relation $k_{rl} = S^3$. The saturation dependency of k_{rg} and k_{rl} are plotted in Fig. 4. The intrinsic permeability and relative permeabilities given in Eqs. (14) and (16) provide the basis for an analysis of moisture transport in partially saturated apple tissues when pressure driven flow is important. These two relationships were used in a comprehensive simulation model to reveal the importance of internal vapor pressure on microwave drying of fried apples (Feng, Tang, Cavalieri, & Plumb, 2001).

5. Conclusions

The experimental procedure developed in this study provided a feasible approach to determine intrinsic and relative permeability of partially saturated apple tissues. The measured intrinsic permeability of Red Delicious apple tissues is in the range of 8.89×10^{-13}–4.57×10^{-11} m^2 for porosity ranging from 0.33 to 0.77. The intrinsic permeability of intact apple tissues (4.57×10^{-11} m^2) compared favorably with literature data for similar bioproducts. The porosity dependency of intrinsic permeability can be described by a Kozeny–Carman model.

Acknowledgements

This project was partially supported by the Washington State University IMPACT Center and Agricultural Research Center, and by the University of Illinois Agricultural Center.

References

Avraam, D. G., & Payatakes, A. C. (1995). Flow regimes and relative permeabilities during steady-state two-phase flow in porous media. *Journal of Fluid Mechanics, 293*, 207–236.

Baijal, S. K. (1982). *Flow behavior of polymers in porous media*. Tulsa, OK: PennWell Books.

Berge, L. I., Gjertsen, L. H., & Lysne, D. (1998). Measured permeability and porosity of R11 (CCl3F) hydrate plugs. *Chemical Engineering Science, 53*, 1631–1638.

Carman, P. C. (1937). Fluid flow through granular beds. *Transactions for Institute of Chemical Engineer, 15*, 150–166.

Choong, E. T., Tesoro, F. O., & Manwiller, F. G. (1974). Permeability of twenty-two small diameter hardwoods growing on southern pine sites. *Wood and Fiber, 6*(1), 91–101.

Couture, F., Jomaa, W., & Puiggali, J.-R. (1996). Relative permeability relations: A key factor for a drying model. *Transport in Porous Media, 23*, 303–335.

Dullien, F. A. L. (1979). *Porous media. Fluid transport and pore structure*. New York: Academic Press.

Eischens, G., & Swanson, A. (1996). Proposed standard test method for measurement of pneumatic permeability of partially saturated porous materials by flowing air. *Geotechnical Testing Journal, 19*(2), 232–239.

Feng, H. (2000). Microwave drying of particulate foods in a spouted bed. Ph.D. thesis, Washington State University.

Feng, H., Tang, J., Cavalieri, R. P., & Plumb, O. A. (2001). Heat and mass transport in microwave drying of porous materials in a spouted bed. *AICHE Journal, 47*(7), 1499–1511.

Goedeken, D. L., & Tong, C. H. (1993). Permeability measurements of porous food materials. *Journal of Food Science, 58*, 1329–1331.

Greenkorn, R. A. (1983). *Flow phenomena in porous media*. New York: Marcel Dekker.

Honarpoor, M., & Mahmood, S. M. (1988). Relative-permeability measurement: An overview. *Journal Petroleum Technology* (August), 963–966.

Johnson, E. F., Bossler, D. P., & Naumann, V. O. (1958). Calculation of relative permeability from displacement experiments. *Petroleum Transactions, AIME*, 370–372.

Krokida, M. K., & Maroulis, Z. B. (1999). Effect of microwave drying on some quality properties of dehydrated products. *Drying Technology, 17*, 449–466.

Lozano, J. E., Rotstein, E., & Urbicain, M. L. (1980). Total porosity and open-pore porosity in the drying of fruits. *Journal of Food Science, 45*, 1403–1407.

Mohsenin, N. H. (1986). *Physical properties of plant and animal materials* (2nd ed.). Netherlands: Gordon and Breach Publishers.

Moldrup, P., Poulsen, T. G., Schjønning, P., Olsen, T., & Yamaguchi, T. (1998). Gas permeability in undisturbed soils: measurements and predictive models. *Soil Science, 163*(3), 180–189.

Nield, D. A., & Bejan, A. (1999). *Convection in porous media* (2nd ed.). New York: Springer.

Ordovás, J., Carmona, E., Moreno, M. T., & Ortega, M. C. (1996). Characteristics of internal porosity of cork container media. *HortScience, 31*(7), 1177–1179.

Perré, P., & Turner, I. (1997). The use of macroscopic equations to simulate heat and mass transfer in porous media: Some possibilities illustrated by a wide range of configurations that emphasize the role of internal pressure. In I. Turner, & A. Mujumdar (Eds.), *Mathematical modeling and numerical techniques in drying technology* (pp. 83–156). New York: Marcel Dekker.

Perré, P., & Turner, I. (1999). A 3-D version of TransPore: A comprehensive heat and mass transfer computational model for simulating the drying of porous media. *International Journal of Heat and Mass Transfer, 42*, 4501–4521.

Plumb, O. A. (1991). Heat transfer during unsaturated flow in porous media. In S. Kakac, B. Kilkis, F. A. Kulacki, & F. Arinc (Eds.), *Convective heat and mass transfer in porous media* (pp. 435–464). Dordrecht: Kluwer Academic Publishers.

Rice, R. W., & D'Onofrio, M. (1996). Longitudinal gas permeability measurements from eastern white pine, red spruce, and balsam fir. *Wood Fiber Science, 28*(3), 301–308.

Roman, G. N., Urbicain, M. J., & Rotstein, E. (1982). Moisture equilibrium in apples at several temperatures: Experimental data and theoretical considerations. *Journal of Food Science, 47*, 1484–1489.

Stylianou, C., & DeVantier, B. A. (1995). Relative air permeability as function of saturation in soil venting. *Journal of Environmental Engineering, 121*(4), 337–347.

Tesoro, F. O., Choong, E. T., & Kimbler, O. K. (1974). Relative permeability and the gross pore structure of wood. *Wood and Fiber, 6*(3), 226–236.